

# Fabricating 3D Structures by Combining 2D Printing and Relaxation of Strain

Brian J. Cafferty, Victoria E. Campbell, Philipp Rothmund, Daniel J. Preston, Alar Ainla, Nicolas Fulleringer, Alina C. Diaz, Alberto E. Fuentes, Dan Sameoto, Jennifer A. Lewis, and George M. Whitesides\*

This paper describes the fabrication of elastomeric three-dimensional (3D) structures starting from two-dimensional (2D) sheets using a combination of direct-ink printing and relaxation of strain. These structures are fabricated in a two-step process: first, elastomeric inks are deposited as 2D structures on a stretched elastomeric sheet, and second, after curing of the elastomeric inks, relaxation of strain in the 2D sheet causes it to deform into a 3D shape. To predict bending of elastomeric objects fabricated with this technique, a simple mechanical model is developed. The strategy of using initially 2D materials to fabricate 3D structures offers four new features that complement digital fabrication techniques. (i) It provides a simple route to create shapes with complex curves, suspended features, and internal cavities. (ii) It is a faster method of fabricating some types of shapes than “conventional” 3D printing, because the features are printed in 2D. (iii) It forms surfaces that can be both smoother, and structured in a way that is not compatible with layer-by-layer processing. (iv) It forms structures that can be deformed reversibly after fabrication by reapplying strain. This paper demonstrates these features by fabrication of helices, structures inspired by cubes and tables, “pop-up” structures, and soft grippers.

The term “3D printing” encompasses additive manufacturing techniques that use one or more translational elements (stage and/or printing heads) that are controlled by a computer to move an ink deposition nozzle, or laser-writing optics, to fabricate a digitally programmable pattern.<sup>[1–7]</sup> In general, these techniques are relatively slow, may require deposition of sacrificial


materials to achieve extreme overhangs, and are limited by trade-offs between the speed of printing and the minimum feature sizes and surface roughness.<sup>[8,9]</sup> In contrast, “2D printing” techniques (such as digital printing and screen printing) are rapid, relatively inexpensive, and routinely achieve sub-millimeter feature sizes.

Nature has also evolved the ability to form complex 3D structures (e.g., leaves, flowers, and tendrils) from initially quasi-planar structures.<sup>[10–15]</sup> These 2D to 3D transformations have inspired the design of synthetic structures that display complex changes in shape when subjected to appropriate stimuli (surface or interfacial stress, edge stress, misfit strain, residual stress, differential growth, swelling, and mechanical instabilities).<sup>[16,17]</sup> These processes also suggest possible routes to micro- and nanoelectromechanical systems (MEMS and NEMS),<sup>[18,19]</sup> and to systems for drug delivery,<sup>[20]</sup> actuation,<sup>[19,21]</sup> microrobotics,<sup>[22,23]</sup> and new materials.<sup>[23,24]</sup> In this paper, we describe a technique to fabricate 3D structures

from planar elastomeric bilayers with mismatched strain that is compatible with digital printing. We determine that a relatively simple set of primitive structures printed on a prestretched 2D sheet can result in a variety of complex 3D objects by producing both positive and negative curvature of whole parts, as well as “pop-up” structures on 2D or 3D sheets.

Dr. B. J. Cafferty, Dr. V. E. Campbell, Dr. P. Rothmund, Dr. D. J. Preston, Dr. A. Ainla, Dr. N. Fulleringer, A. C. Diaz, A. E. Fuentes, Prof. G. M. Whitesides  
Department of Chemistry and Chemical Biology  
Harvard University  
12 Oxford Street, Cambridge, MA 02138, USA  
E-mail: gwhitesides@gmwgroup.harvard.edu  
Dr. P. Rothmund, Prof. J. A. Lewis  
School of Engineering and Applied Sciences  
Harvard University  
29 Oxford Street, Cambridge, MA 02138, USA

Dr. P. Rothmund, Prof. G. M. Whitesides  
Kalvi Institute for Bionano Science and Technology  
Harvard University  
29 Oxford Street, Cambridge, MA 02138, USA  
Prof. D. Sameoto  
Department of Mechanical Engineering  
University of Alberta  
9211 116 Street NW, Edmonton, AB T6G1H9, Canada  
Prof. J. A. Lewis, Prof. G. M. Whitesides  
Wyss Institute for Biologically Inspired Engineering  
60 Oxford Street, Cambridge, MA 02138, USA

 The ORCID identification number(s) for the author(s) of this article can be found under <https://doi.org/10.1002/admt.201800299>.

DOI: 10.1002/admt.201800299

The study of structural elastic instabilities in soft materials has experienced a resurgence in interest, in part, due to studies of buckling.<sup>[25–30]</sup> Buckling of rigid materials (metals, concrete, etc.) usually leads to permanent damage, and is thus usually regarded as a mechanism of failure in structural materials.<sup>[31]</sup> Buckling of soft materials (elastomers, foams, some gels, etc.), however, leads to quite different outcomes if it is largely or exclusively reversible on removal of the force that caused it to buckle.<sup>[32–34]</sup> These elastic instabilities offer a new form of actuation. For example, buckling, as a design principle, has been used to actuate soft robots,<sup>[33,34]</sup> to make tunable metamaterials,<sup>[35–37]</sup> to fabricate complex micro/nanomaterials,<sup>[38–43]</sup> and control adhesive surfaces.<sup>[44,45]</sup> We have demonstrated that reversible buckling of elastomeric beams may be employed for torsional soft actuators by applying negative pressure to an elastomeric structure made of interconnected cavities that reversibly deform,<sup>[33]</sup> and for linear actuators inspired by muscle.<sup>[34]</sup>

Buckling instabilities and bending due to compressive in-plane stresses in 2D sheets may be used to generate 3D shapes.<sup>[38,46–53]</sup> These compressive stresses can result, for example, from swelling of an inhomogeneous hydrogel,<sup>[46]</sup> or from selective swelling of a homogeneous hydrogel using a mask.<sup>[47]</sup> With these approaches, however, it is difficult to control the final shape of the structures because the hydrogels can buckle to either side of the sheet.<sup>[47]</sup> This symmetry problem can be solved using bilayers in which one layer expands or contracts more than the other layer. In these systems, the structure of the bilayer controls the direction of bending, which provides a way to design desired shapes accurately (e.g., bistable and helical structures).<sup>[11,54]</sup> Inspired by plants with shape-changing structures caused by anisotropic swelling of fibers,<sup>[24]</sup> bending of bilayers using anisotropic swelling has been demonstrated with hydrogels of different stiffness.<sup>[55]</sup> The bending deformation of a bilayer composed of two metals with different coefficients of thermal expansion has most frequently been used to measure temperature,<sup>[56]</sup> and bilayers consisting of one passive layer and one layer that responds to a stimulus have been used for actuators and robots.<sup>[21,57,58]</sup> Bilayers may also form 3D structures when materials with “mismatching” strain or internal stress are bonded to one another. For example, bonding a stretched elastomeric material to an unstretched elastomeric material will cause bending in the resulting bilayer due to residual stresses.<sup>[11,30,53,54,59]</sup> This concept has also been applied at the nanoscale: when two thin layers of materials with different lattice constants are deposited on a substrate, the bilayer “rolls” into a nanotube upon release from the substrate.<sup>[60]</sup>

This paper demonstrates the fabrication of 3D structures by printing 2D polymer precursors, on prestrained elastomeric sheets. When the strained elastomers are released, they bend or buckle into 3D structures due to relaxation of strain in the stretched elastomeric sheets. This strategy—using initially 2D materials to fabricate 3D shapes—offers capabilities that complement more familiar fabrication techniques (molding, digital printing), in specific applications, for four reasons. (i) It provides a simple route to shapes with complex curves, suspended features, and internal cavities (without the use of sacrificial materials), features that are difficult to make by these techniques. (ii) It can be faster than techniques used for fabrication in three dimensions. (iii) It produces surfaces that

can be smoother than those produced using layer-by-layer processing. (iv) It produces structures that can be deformed reversibly by reapplying strain, which can be used to fabricate more complex structures and actuators. This approach differs from prior work, in which strain relaxation formed buckled “pop-up” structures on flat elastomeric substrates,<sup>[53,61,62]</sup> in that the approach described here allows the entire composite structure, including the substrate, to be fabricated with positive or negative curvature.

We control the final shape of the elastomeric objects by controlling five parameters: (i) the magnitude and anisotropy of the stretching of the preformed elastomeric sheet and the shape of the sheet; (ii) the thickness of the deposited ink relative to the thickness of the elastomeric sheet; (iii) the pattern of the printed elastomeric ink; (iv) the pattern of adhesive and non-adhesive regions on the sheets; and (v) the mechanical properties of both the sheet and printed elastomers. To print the 2D designs on to stretched elastomers, we either used a TEVO Tarantula Prusa-i3 printer that we customized to print elastomeric silicone inks (Figures S1–S3, Supporting Information), or we printed the inks manually. To control the thickness of the printed lines, we extruded the elastomeric ink from blunt-ended needles with gauges that ranged from 14 (inner diameter: 1.54 mm) to 32 (inner diameter: 0.1 mm). To control the speed of printing, we changed the value of the lateral translation speed of the printer head; we used values that ranged from 5 to 30 mm s<sup>-1</sup>. Unless otherwise noted, we used Dragon Skin 10 SLOW to make the sheets, strips, and elastomeric inks. We derive a model to describe the bending of the bilayer, and illustrate the fabrication of elastomeric helices, structures inspired by cubes and tables, and soft grippers.

We first studied the bending behavior of hyperelastic bistrisps because they provide a simple and idealized model to study the bending of elastic systems. These bistrisps consist of two elastic strips of different lengths (Figure 1). The shorter strip (labeled 1 in Figure 1a) of length  $L_1$  is longitudinally stretched to match the length of the longer strip (labeled 2 in Figure 1a) of length  $L_2$  (i.e., stretch  $(\lambda_p) = L_2/L_1$ ), and the longer strip is attached to the shorter strip at their interface. Upon release, the bistrisp bends to minimize its elastic energy. In the final state, the shorter strip is under tensional stress and the longer strip under compressive stress. Although hyperelastic bistrisps have been studied extensively, all previously reported hyperelastic bistrisp systems have been fabricated by gluing together two preformed elastomers.<sup>[11,30,54,59]</sup> We fabricated the bistrisps by stretching the shorter strip, and then we extruded uncured elastomer onto the stretched strip (Figure 1b), which, after curing, forms the longer strip—a process that is compatible with 2D printing techniques. After curing the elastomer, we release the bistrisp to allow it to curl into the final shape (Figure 1b). Unlike bistrisps formed from two different materials, this method allows the curvature to be independent of temperature, because both layers are the same material.

We used silicone elastomer strips with width  $W_1 = 5$  mm, and thickness  $t_1 = 2$  mm. We stretched these strips by six different stretches  $(\lambda_p = 1.0, 1.1, 1.3, 1.5, 1.8, \text{ and } 2.4)$ . On the stretched strips, we deposited, using a modified 3D-printer, a layer of elastomeric precursor composed of the same material (thickness  $t_2 = 0.2, 0.4, \text{ and } 0.6$  mm). We cured the

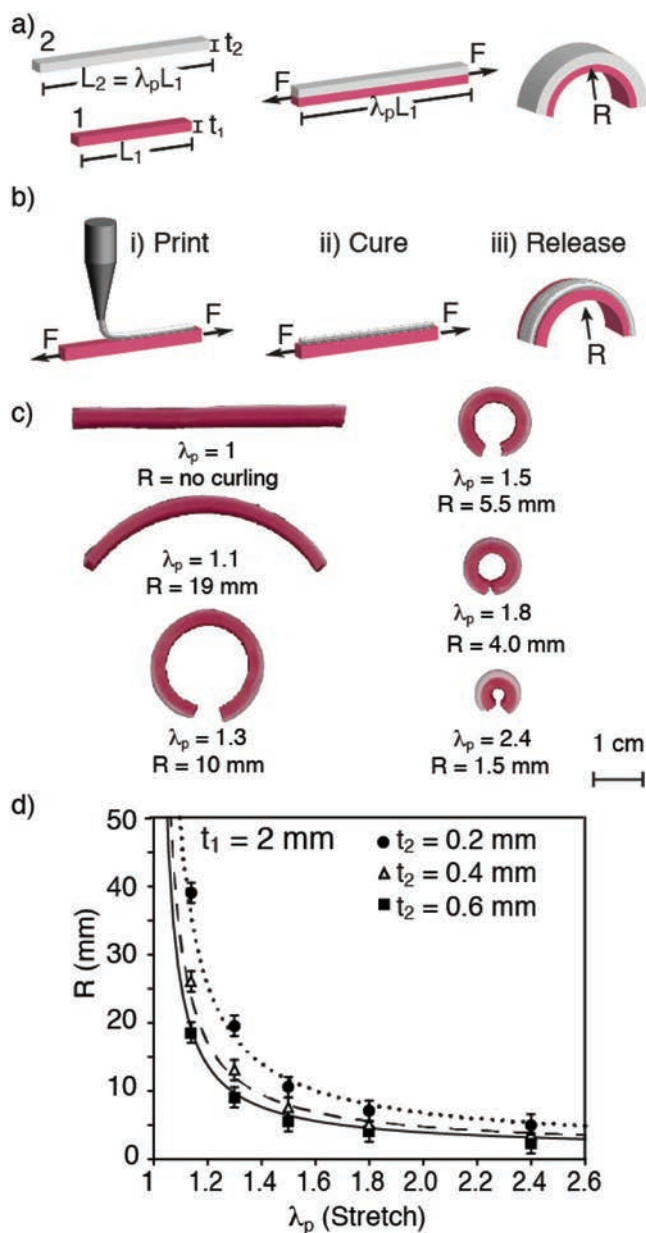


**Figure 1.** a) Illustration depicting formation of a hyperelastic bistrip. Strip 1 (pink) of initial length  $L_1$ , and thickness  $t_1$ , is stretched to a final length of  $\lambda_p L_1$  (middle), and attached to strip 2 (white). Strip 2 has uncompressed dimensions of length  $L_2 = \lambda_p L_1$ , and thickness  $t_2$ . Upon release, the bilayer curves to minimize its energy (right). b) Illustration depicting the method used to fabricate a bistrip in this work: (i) an elastomeric strip (ink) was printed on a strained elastomeric strip; (ii) the printed strip was cured; and (iii) the bistrip was released, and curved spontaneously. c) Photographic images of curved bilayer structures obtained by fabricating bistrips at six different values of  $\lambda_p$ . The bistrips had a value of  $t_1$  of 2 mm and a value of  $t_2$  of 0.6 mm. The bistrips with values of  $\lambda_p$  of 1.5, 1.8, and 2.4 were cut for clarity to show the curvature of the beam. Larger values of  $\lambda_p$  correspond to greater curvature. d) Plot of  $\lambda_p$  versus the radius of curvature ( $R$ ) at constant  $t_1$  (2 mm), and three values of  $t_2$  (0.2, 0.4, and 0.6 mm). The lines represent the values obtained from the analytical model. Reported values are mean  $\pm$  S.D. ( $n = 7$  measurements).  $\lambda_p$  is the stretch ( $\lambda_p = L_2/L_1$ ),  $t_1$  is the thickness of the stretched elastomer prior to stretching,  $t_2$  is the thickness of the printed elastomer after curing.

bistrip at 80 °C for 3 min. Figure 1c shows photographic images of the curved bistrips obtained with  $t_2 = 0.6$  mm and different values of  $\lambda_p$ . For  $\lambda_p = 1$  (i.e., the elastomeric strip was not stretched), the bistrip did not curl. With increasing  $\lambda_p$ , the radius of curvature ( $R$ ) of the final structures decreased to  $R = 1.5$  mm when  $\lambda_p = 2.5$ . The thickness of the printed elastomer can also be used to control the magnitude of the resulting curvature. Thinner printed layers led to larger values of  $R$  at the same stretch (Figure 1d and Table S1, Supporting Information), because the constraint on the deformation of the first strip was smaller.

To understand the mechanical behavior of the bistrip, we developed a simple model. When the width, and the material of both strips are the same, the radius of curvature depends only on the thicknesses of the two layers ( $t_1$  and  $t_2$ , mm) and the stretch ( $\lambda_p = L_2/L_1$ ). In this case, the radius of curvature of the bilayer can be described with a function  $g$  that only depends on two nondimensional parameters (Equation (1))

$$R/t_1 = g(\lambda_p, t_1/t_2) \quad (1)$$

Based on these parameters, we modeled the bistrip as an Euler–Bernoulli beam using the hyperelastic, incompressible neo-Hookean material model.<sup>[63,64]</sup> The function  $g$  cannot be obtained analytically. To obtain  $R$  we therefore minimized the energy of deformation of the entire structure numerically (see Figure S4 and the Supporting Information for a detailed description of the model). The values predicted by the model are in excellent agreement with the values we obtained from our experiments (Figure 1d). When the bistrips are the same material, this model relies solely on geometrical parameters, and may therefore be used to design 3D structures with accurate prediction of the final shape.

We can form helices if the circumference of the curved bistrip is smaller than the deformed length of the strip ( $L_1$ ). When this condition is satisfied, joining a stretched elastic strip side-by-side to another elastic strip and releasing it will spontaneously form periodic helical sections of alternating chirality that are separated by perversions (a type of structure that has also been referred to as a hemihelix).<sup>[11,30]</sup> A continuous helix can, alternatively, be formed if one of the ends of the bistrip is twisted after it is released from the support.<sup>[11]</sup> We examined if bistrips that are formed from printing an elastomer onto a stretched elastomeric strip could generate these structures.

We fabricated both elastomeric helices and hemihelices by printing on stretched elastomeric strips (Figure 2). Upon releasing the bistrip, it compressed and twisted out of plane to minimize its energy, and thus coiled into a helix. We tuned the radius of curvature ( $R$ ) by changing the stretch (larger  $\lambda_p =$  smaller  $R$ ) and the thickness of the printed elastomer. Figure 2d shows a plot of the load (N) as a function of elongation (mm) for the two configurations. For the hemihelical configuration, which also exhibits elastic behavior, there is a conformational transition at 0.36 N between the coiled and the straight geometries of the hemihelix. This transition translates to a change in the slope of the curve (at the kink) indicating a stiffening of the structure (the transition is more gradual for the helical configuration). Because the helices and hemihelices are made of elastomeric materials, they

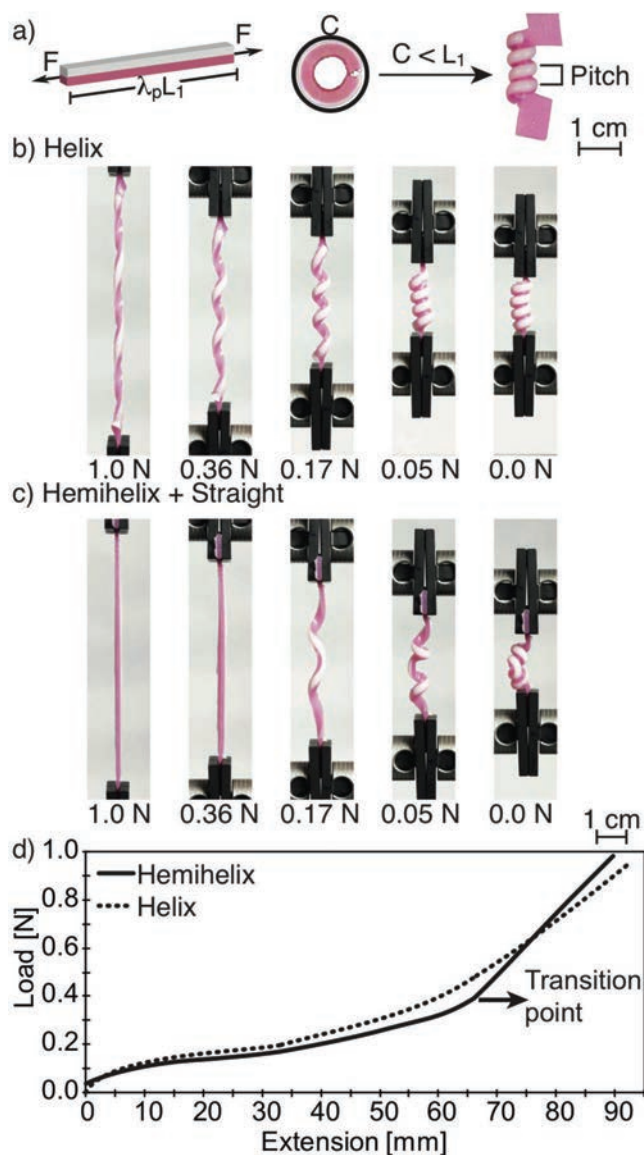


**Figure 2.** a) Schematic representation of the fabrication of the springs. Left: the bistrip system in the strained configuration. Middle: photographic image of a curved bistrip system;  $C$  = circumference. When  $C < L_1$  the unstretched bistrip bends out of plane and coils. Right: photographic image of the coil. b) Photographic images of a helical spring under tension. c) Photographic images of a hemihelical spring under tension. The elastomeric spring will regain its initial configuration after full extension. d) Plot of load as a function of extension for the helical and hemihelical configurations. The transition point is caused by the material transitioning from partially coiled to uncoiled (linear).

can sustain large deformations without damage, that is, the springs will return to their initial conformation even after being stretched completely into a linear geometry (Figure 2b,c and the Supporting Information for materials properties). We repeated this stretch/release cycle 1000 times, and measured the stress-strain curves of the springs. The materials did not show signs of degradation (Figure S5, Supporting Information).

We can extend this fabrication technique from 1D strips to 2D sheets. 3D structures, such as arcs and waves, have been

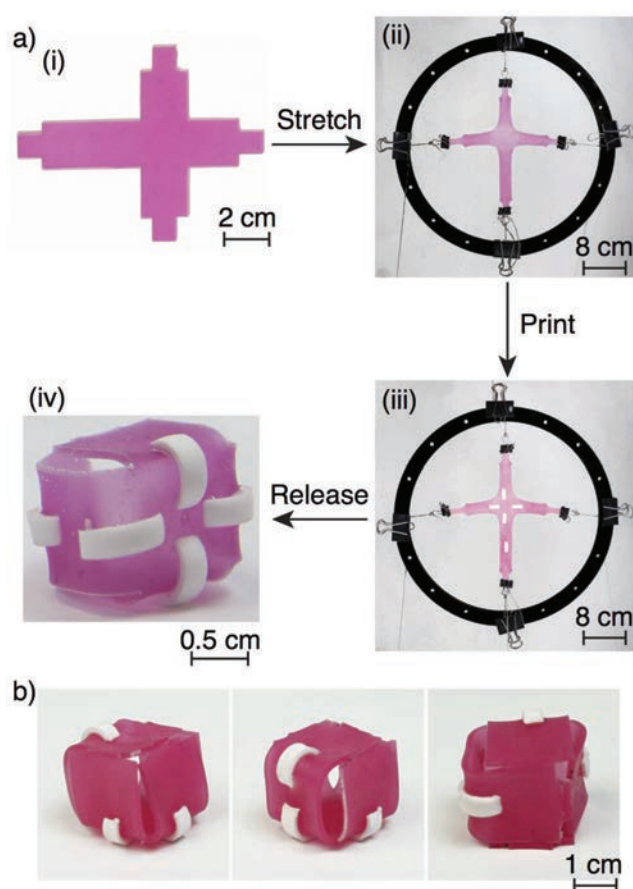


**Figure 3.** a) Photographic images of the fabrication process for making an elastomeric quasi-cube: (i) flat elastomeric sheet; (ii) the sheet was stretched using a custom-built support; (iii) an elastomeric ink was printed on the stretched sheet; (iv) the sheet was released from the support, generating the 3D structure (a cube). b) Photographic images of the cube-like object.

made using strain relaxation of 2D sheets;<sup>[53,61]</sup> these structures, however, do not incorporate the 2D sheet in their final 3D form, due, in part, to large differences in the thickness of the two layers. Because the approach described here uses a base layer and a printed layer that have the same elastic modulus (as they are made from the same elastomer) and thicknesses that are on the same order of magnitude, this approach can be used to fabricate structures in which the entire composite material has a curvature. **Figure 3** shows the fabrication of a structure topographically similar to a cube. The 2D elastomeric sheet was cut into a planar representation of a cube. Using a custom-built support, we stretched the sheet in perpendicular directions. As with the bistrip model system (Figure 1), the final curvatures of the hinges of the cube depend on the amount of stretching imposed on the elastomeric sheet (for this cube,  $\lambda_p = 1.2$ ). Using a stencil, we printed the elastomeric lines with a  $t_2$  of 2 mm,  $L_2$  of 15 mm, and width ( $W_2$ ) of 5 mm, onto the stretched 2D sheet and allowed the printed strips to cure. After releasing the structure from the support and placing it in a water bath (to reduce friction, and to minimize the effect of gravity), we obtained an object with roughly cubical shape.

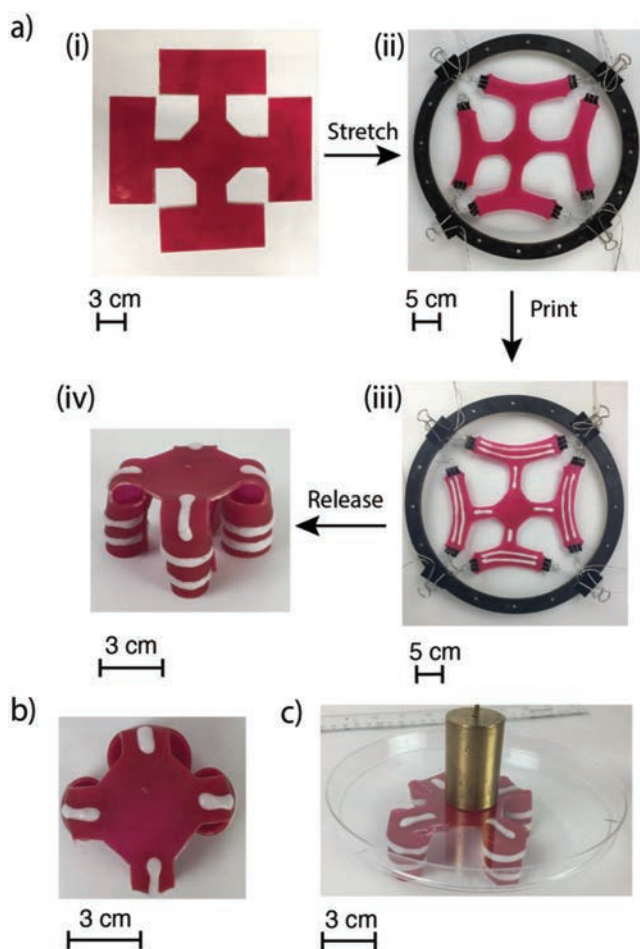


**Figure 4.** a) Photographic images of the fabrication process for making an elastomeric “table”: (i) a flat elastomeric sheet was cut into a 2D representation of a table; (ii) the sheet was stretched using a support; (iii) an elastomer ink was printed on the stretched sheet; (iv) the sheet was released generating the 3D structure (a “table”). Photographic images showing b) the top of the “table,” and c) the “table” supporting a plastic petri dish and a 200 g weight.

**Figure 4** shows another proof-of-concept demonstration, the fabrication of an elastomeric “table.” We fabricated the table using the same support and similar design process used to form the cube. For this structure, four sets of elastomeric lines were printed perpendicular to each other, one set of lines formed hinges at the base of the legs of the “table” ( $t_2 = 2$  mm,  $L_2 = 10$  mm, and  $W_2 = 5$  mm) and the other set of lines formed curled substructures that serve as the “legs” ( $t_2 = 2$  mm,  $L_2 = 100$  mm, and  $W_2 = 5$  mm). The amount of bending of the hinges and the legs of the table was determined by the stretch (for this table,  $\lambda_p = 1.5$ ). The table in this demonstration weighed 18 g and could support 200 g (Figure 4c).

Inspired by a shape-morphing carnivorous plant, *Dionaea muscipula* (commonly known as Venus flytrap), we designed and fabricated grippers (Figure 5) that—given that the material is soft—are able to conform to complex, fragile asymmetric shapes (in these examples the forms were two cherries, and a Madagascar hissing cockroach—chosen because it is a living insect that is remarkably passive physically).

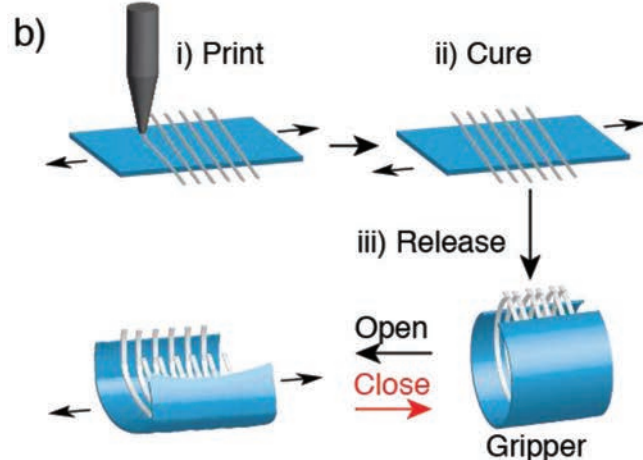
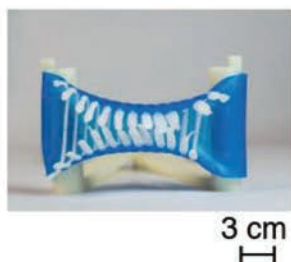
We made this gripper in four steps. (i) We stretched an elastomer sheet. The sheet shown in Figure 5a has dimension of  $t_1 = 2$  mm,  $W_1 = 35$  mm, and  $L_1 = 60$  mm. The sheet was stretched in an axial direction (for this gripper,  $\lambda_p = 2.4$ ). (ii) We printed elastomeric lines of  $t_2 = 0.4$  mm and  $W_2 = 2$  mm. (iii) The lines were cured at 80 °C on the printer build-bed. (iv) To obtain the gripper, we released the flat sheet. Unlike the previous demonstrations where the bilayer bends away from the printed lines, here the sheet bends toward the printed lines. This difference reflects the fact that when we stretched the sheet axially in step (i), it contracted perpendicular to the direction of stretch. Because the printed lines were almost perpendicular to the stretching direction, layer 1 was compressed (instead of stretched) in the direction the lines were printed.

The gripper opens and closes by pulling (and releasing) the gripper in the direction of strain using a handle to which the gripper is attached. This gripper is able to conform to asymmetric shapes and can pick up multiple objects simultaneously. Figure 5c,d shows photographic images of the same gripper picking up two cherries that weighed 12 and 13 g each, and a live cockroach. These examples demonstrate that the gripper is adaptable to different geometrical conformations, and that it is compatible with delicate objects: it did not damage the cherries or the cockroach. To tune the strength of the gripper, we employed different materials to fabricate the sheet and the extensions (the “fingers”) of the elastomeric material. As summarized in Table S2 (Supporting Information), the grippers can lift objects of different shapes and sizes, such as flowers, stainless steel spheres, and glass vials.

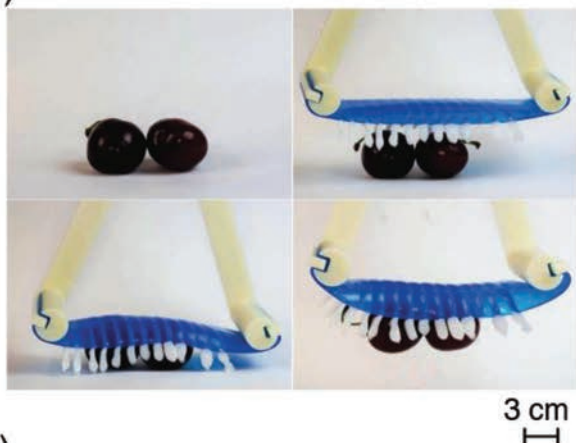
Recently, Wang and co-workers reported the fabrication of “pop-up” structures on a planar elastomeric textile substrate (Spandex) using a process that includes selective bonding and relaxation of strain in the substrate.<sup>[53]</sup> We have used the approach described in this work to fabricate similar “pop-up” structures with the characteristic that the ink and elastomeric sheet are not continuously attached. Specifically, we use a release agent and pre patterning of the stretched sheet to define regions where the ink, once it is cured, will and will not adhere to the strained sheet. Figure S6 (Supporting Information) shows an example of the fabrication of a buckled eight-petal structure that we made in five steps. (i) Using a custom-built support, we uniformly stretched a circular elastomeric sheet to obtain a value of  $\lambda_p = 1.7$ . This sheet measured 2 mm in thickness, and 100 mm in diameter before stretching. (ii) Onto this stretched sheet, we placed a mask to define eight points of adhesion, and covered the protected sheet with mold release (Ease Release 200). This action generated regions of “protected” surface where the ink could not adhere, and regions of “unprotected” surface where the ink could adhere. The positions coated in mold release were small (5 mm × 5 mm) in order to minimize bending of the elastomeric sheet after it was released. (iii) We printed a circular pattern, which coated both the “protected” and “unprotected” regions. (iv) We cured the ink by heating the support to 80 °C. (v) Upon releasing the sheet, an eight-petal pattern was formed.

Expanding on the technique of patterning regions of adhesion and nonadhesion using a release agent, we fabricated a pneumatic gripper with a three-finger design (Figure 6). Grippers made from elastomeric material and actuated pneumatically

a) Gripper



c)



d)

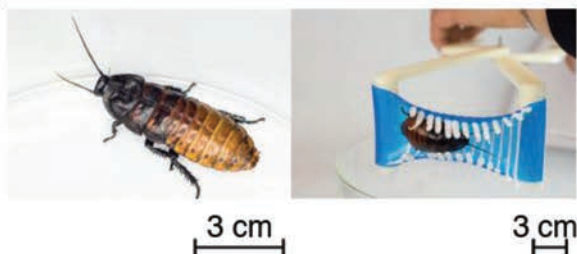


**Figure 5.** a) Photographic image of a gripper attached to the handle. b) Schematic representation of the fabrication steps of the mechanically actuated gripper: (i) elastomeric ink was printed on a stretched elastomeric sheet at a 60° angle relative to the direction of the stretch; (ii) the elastomeric ink was cured; (iii) the gripper was released from the support and attached to a handle to actuate its movement. c) Photographic images of the gripper picking up two cherries that weighed 11.5 and 13.2 g.

have previously been shown to close in the activated state (i.e., when pressurized);<sup>[65]</sup> this gripper, however, is closed in the relaxed state and opens when activated. Figure 6a shows the process used to fabricate this gripper. Here, an elastomeric sheet (2 mm thick), cut in a 2D representation of the three-finger gripper, was stretched on a support to obtain a value of  $\lambda_p = 1.5$ . The edges of the sheet were covered with a mask to protect the outermost surface of the sheet, and mold release was coated on the exposed surface of the stretched elastomer. The mask was removed and uncured elastomer was applied on both the protected and unprotected areas, within a stencil, which was used to obtain a top layer with a consistent height of 1.5 mm. The top layer was cured, released from the support, and a tube was inserted into the center of the gripper to fill the air compartments that were formed at the positions where the mold release was applied. The gripper could pick up objects with a variety of different shapes, including a ping-pong ball, a glass beaker containing two rubber balls (weighing a total of 45 g), and a plastic cup containing five rubber balls (weighing a total of 69 g).

In summary, we have demonstrated a simple strategy for the design and rapid fabrication of nonplanar (3D) structures starting from strained planar (2D) elastomeric strips or sheets. We obtain these structures using a printer that was customized to print elastomeric polymeric features (threads, lines, and rectangles) instead of printing rigid thermoplastic polymers, or by manually printing these elastomeric inks onto stretched elastomeric sheets. We present a simple analytical model of the mechanics of bending induced by stretching, and show that we can control the bending by controlling the amount of strain and/or the thickness of the printed elastomer deposited on the strips and sheets. Although the structures that we fabricated to illustrate this work were composed of a single, commercially available elastomer, similar principles with different elastomers, or with composites of elastomers and sheets that bend but do not stretch can also be used. Optimization of material properties and thicknesses of the layers could enable more mechanically stable materials to be incorporated in this method.

Because this technique is compatible with 2D printing methods (digital printing, screen printing), and avoids the time-consuming multiple passes of printing required by standard 3D printing methods, it could be used to fabricate structures that are not compatible (or easily obtained) with layer-by-layer processing, and could also provide a relatively fast method of prototyping 3D objects. Through both the mechanically actuated and pneumatically actuated soft grippers, we show that this technique can be used in the fabrication of soft robots; in both of these demonstrations the bending of the bilayers, which was formed as a result of mismatched strain in the two elastomeric layers, was integral for actuation of the grippers. This technique can thus be adapted to a number of technologies that desire rapid printing and/or the fabrication of structures with compliant and reversible features.

d) Photographic image of a Madagascar hissing cockroach, and an image of the gripper picking up the cockroach. The schematic drawings in (b) are approximate and do not represent the complex distortion of the structure on stretching.

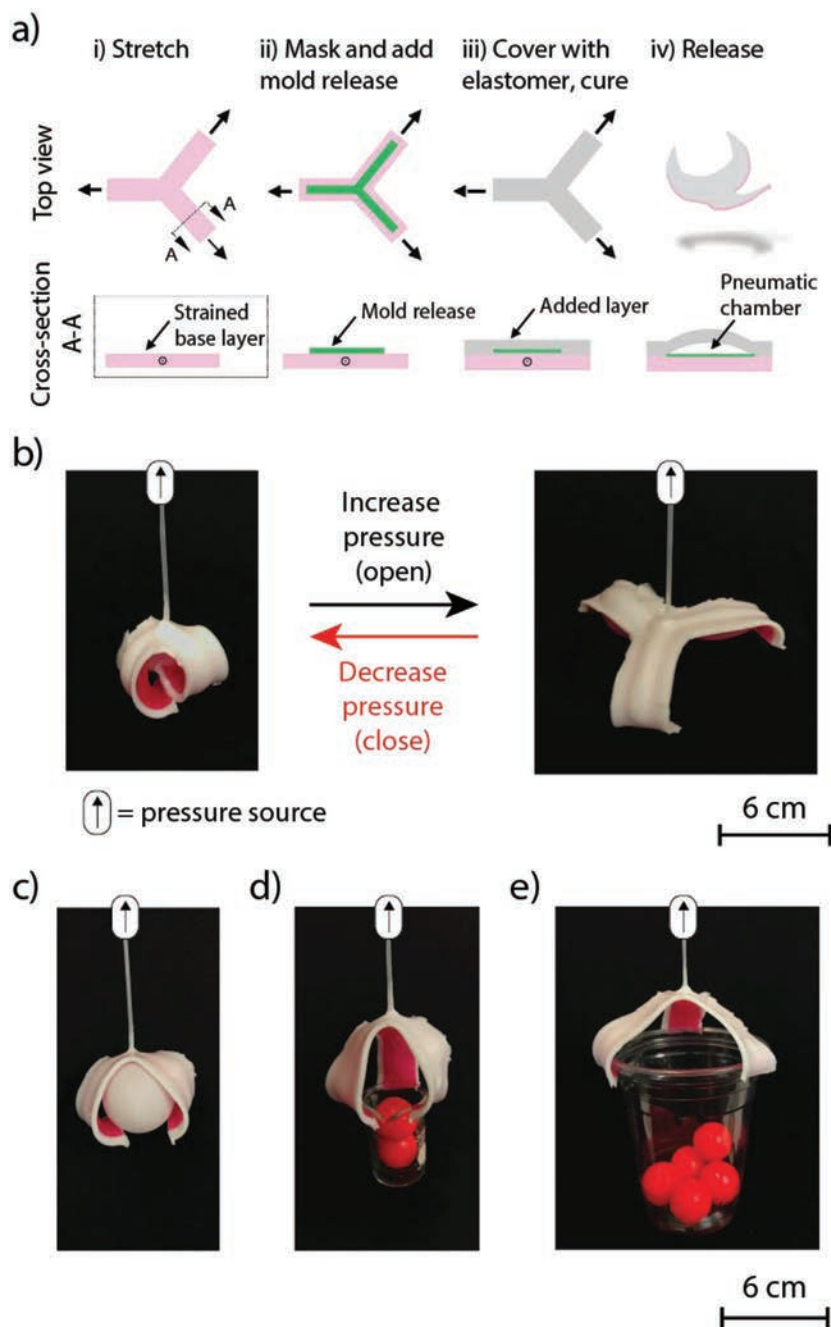


**Figure 6.** a) Schematic representation of the fabrication steps of the pneumatically actuated gripper: (i) a flat elastomeric sheet (pink) was cut into a 2D base layer for the gripper and stretched using a support; (ii) the edges of the elastomer were covered using a mask, the exposed surface was covered with mold release (green), and the mask was removed; (iii) using a stencil, elastomeric ink (white) was printed on both the area coated with mold release and the area that was uncoated, and this elastomeric layer was cured; (iv) the resulting bilayer was released from the support, relaxation of strain in the bilayer caused the top layer to buckle at positions where mold release was applied, and these positions formed the pneumatic chamber. A tube was inserted in the center of the gripper to inflate it. The process is shown from two perspectives; the top view shows the process orthogonal to the surface of the sheet, and cross-section A-A shows a cross section of one of the legs of the sheet (demarcated by dashed lines in part (i)). b) Images of the gripper in the relaxed (closed) and activated (open) states. The gripper was actuated using a 60 mL polypropylene syringe as the source of pressure. Images show the gripper picking up objects with a variety of different shapes, including d) a ping-pong ball, e) a beaker containing two rubber balls, and f) a plastic cup containing five rubber balls.

## Experimental Section

**Materials:** All silicones and pigments were purchased from Smooth-On, Inc. To prepare elastomeric strips and sheets, Dragon Skin 10 SLOW (DS10) was used. To tune the material properties of the gripper, four elastomers (separately and in combination) with different mechanical properties (Shore hardness) were used: Dragon Skin 10 and 30, Ecoflex 00-30, and Smooth-Sil 960. These elastomers are platinum-catalyzed silicone rubbers, and adhere seamlessly to each other. To aid in the visualization of the bilayers, red and white pigments (Silc Pig) were added to the silicones of the stretched sheet and to the printed layer, respectively.

**Fabrication of 3D Structures:** A bistrup hyperelastic system that consisted of elastomeric strips of fixed width (5 mm) and thickness (2 mm), and of different initial lengths was prepared. Elastomeric sheets were formed that were 28 cm × 28 cm with a thickness of 2 mm. Elastomeric strips and sheets were cut using a laser cutter into defined 2D patterns. A custom-built support was made to stretch the cut strips and sheets. Values of stretch between 1.5 and 2.5 were chosen to maintain linear elastic performance of the elastomers (Figure 1d). Onto these stretched strips and sheets, elastomeric ink (made of the same material as the stretched elastomer) was printed that acted as the second layer of the bilayer system (Figure 1). For the “pop-up” structure and pneumatic gripper, mold release (Ease Release 200) was used to define regions of nonbonding between the two layers. 2D designs were made using Adobe Illustrator, exported them to Inkscape (an open source software), and used Inkscape to generate GCode (a numerical control language that the printer can read).

**Printer:** A TEVO Tarantula Prusa-i3 printer customized to print elastomeric silicone inks was used (Figures S1 and S2, Supporting Information). This printer was chosen for four reasons: (i) It is based on the RepRap (replicating rapid prototyper) design, which is an open design project (i.e., all blueprints, and software produced by the RepRap project are released under a free licensing agreement). (ii) Both the software and hardware are easily customizable. (3) It is inexpensive (<\$300 from 3dprintersonlinestore.com). (4) It is equipped with a heated print stage, which decreased the time required to cure the silicone elastomer. The printer is equipped with a thermoplastic extruder nozzle. As it is delivered, the types of structural thermoplastics that the printer can print are rigid, break when subjected to compressive force, and have poor adhesion to the stretched silicone elastomers that were used. To print elastomeric silicone inks, this extrusion nozzle was exchanged for a custom-built syringe pump that used a stepper motor (SparkFun, 39HY34-0404AL), which was compatible with the TEVO Tarantula motor controller, to move the plunger of the syringe. All 3D printed parts were printed in ABS using a Dimension Elite (StrataSys). CAD files used to fabricate the 3D printed parts (Figure S3, Supporting Information) are provided separately in the Supporting Information.

## Supporting Information

Supporting Information is available from the Wiley Online Library or from the author.

## Acknowledgements

B.J.C. and V.E.C. contributed equally to this work. The authors wish to thank Dr. Navneet Bhalla and Dr. Lee Belding for discussions. This work was funded by DOE Award No ER45852. B.J.C. acknowledges partial salary support from the Simons Foundation under Award No. 290364. A.A. thanks the Swedish Research Council (VR) for a postdoctoral fellowship. N.F. acknowledges salary support from BASF. D.S. thanks the Natural Sciences and Engineering Research Council of Canada (NSERC). A.C.D. and A.E.F. acknowledge the Harvard REU program supported by NSF Award No. DMR 1420570.

## Conflict of Interest

George M. Whitesides is on the board of directors of, and owns equity in, Soft Robotics Inc.

## Keywords

3D printing, bilayers, controlled buckling, soft grippers, strain relaxation

Received: July 24, 2018

Published online: August 21, 2018

- [1] J. R. Raney, J. A. Lewis, *MRS Bull.* **2015**, *40*, 943.
- [2] X. Zhang, X. Jiang, C. Sun, *Sens. Actuators, A* **1999**, *77*, 149.
- [3] H. Kodama, *Rev. Sci. Instrum.* **1981**, *52*, 1770.
- [4] J. A. Lewis, *Adv. Funct. Mater.* **2006**, *16*, 2193.
- [5] R. D. Farahani, M. Dubé, D. Theriault, *Adv. Mater.* **2016**, *28*, 5794.
- [6] H. Lipson, M. Kurman, *Fabricated: The New World of 3D Printing*, Wiley, New York **2013**.
- [7] I. Gibson, D. Rosen, B. Stucker, *Additive Manufacturing Technologies Rapid Prototyping to Direct Digital Manufacturing*, Springer, Berlin **2010**.
- [8] M. Mahesh, Y. S. Wong, J. Y. H. Fuh, H. T. Loh, *Rapid Prototyping J.* **2004**, *10*, 123.
- [9] B. N. Turner, R. Strong, S. A. Gold, *Rapid Prototyping J.* **2014**, *20*, 192.
- [10] D. W. Thompson, *On Growth and Form*, Cambridge University Press, Cambridge **1942**.
- [11] J. Liu, J. Huang, T. Su, K. Bertoldi, D. R. Clarke, *PLoS One* **2014**, *9*, e93183.
- [12] Y. Forterre, J. Dumais, *Science* **2011**, *333*, 1715.
- [13] S. Armon, E. Efrati, R. Kupferman, E. Sharon, *Science* **2011**, *333*, 1726.
- [14] J. L. Silverberg, R. D. Noar, M. S. Packer, M. J. Harrison, C. L. Henley, I. Cohen, S. J. Gerbode, *Proc. Natl. Acad. Sci. USA* **2012**, *109*, 16794.
- [15] W. K. Silk, *Environ. Exp. Bot.* **1989**, *29*, 95101.
- [16] X. Yu, L. Zhang, N. Hu, H. Grover, S. Huang, D. Wang, Z. Chen, *Appl. Phys. Lett.* **2017**, *110*, 091901.
- [17] J. H. Pikul, S. Li, H. Bai, R. T. Hanlon, I. Cohen, R. F. Shepherd, *Science* **2017**, *358*, 210.
- [18] J. S. Bunch, A. M. Van Der Zande, S. S. Verbridge, I. W. Frank, D. M. Tanenbaum, J. M. Parpia, H. G. Craighead, P. L. McEuen, *Science* **2007**, *315*, 490.
- [19] E. Smela, O. Inghanas, I. Lundstrom, *Science* **1995**, *268*, 1735.
- [20] J. Wang, K. Liu, R. Xing, X. Yan, *Chem. Soc. Rev.* **2016**, *45*, 5589.
- [21] M. M. Hamed, V. E. Campbell, P. Rothemund, F. Güder, D. C. Christodouleas, J. F. Bloch, G. M. Whitesides, *Adv. Funct. Mater.* **2016**, *26*, 2446.
- [22] S. Felton, M. Tolley, E. Demaine, D. Rus, R. Wood, *Science* **2014**, *345*, 644.
- [23] Z. Tian, L. Zhang, Y. Fang, B. Xu, S. Tang, N. Hu, Z. An, Z. Chen, Y. Mei, *Adv. Mater.* **2017**, *29*, 1604572.
- [24] A. S. Gladman, E. A. Matsumoto, R. G. Nuzzo, L. Mahadevan, J. A. Lewis, *Nat. Mater.* **2016**, *15*, 413.
- [25] N. Hu, R. Burgueño, *Smart Mater. Struct.* **2015**, *24*, 063001.
- [26] S. Yang, K. Khare, P. C. Lin, *Adv. Funct. Mater.* **2010**, *20*, 2550.
- [27] X. Chen, J. Yin, *Soft Matter* **2010**, *6*, 5667.
- [28] K. Bertoldi, V. Vitelli, J. Christensen, M. van Hecke, *Nat. Rev. Mater.* **2017**, *2*, 17066.
- [29] S. H. Kang, S. Shan, A. Kosmrlj, W. L. Noorduin, S. Shian, J. C. Weaver, D. R. Clarke, K. Bertoldi, *Phys. Rev. Lett.* **2014**, *112*, 098701.
- [30] J. Huang, J. Liu, B. Kroll, K. Bertoldi, D. R. Clarke, *Soft Matter* **2012**, *8*, 6291.
- [31] F. S. Merritt, J. T. Ricketts, *Building Design and Construction Handbook*, Vol. 13, McGraw-Hill, New York **2001**.
- [32] P. M. Reis, *J. Appl. Mech.* **2015**, *82*, 111001.
- [33] D. Yang, B. Mosadegh, A. Ainla, B. Lee, F. Khashai, Z. Suo, K. Bertoldi, G. M. Whitesides, *Adv. Mater.* **2015**, *27*, 6323.
- [34] D. Yang, M. S. Verma, J. H. So, B. Mosadegh, C. Keplinger, B. Lee, F. Khashai, E. Lossner, Z. Suo, G. M. Whitesides, *Adv. Mater. Technol.* **2016**, *1*, 1600055.
- [35] M. K. Blees, A. W. Barnard, P. A. Rose, S. P. Roberts, K. L. McGill, P. Y. Huang, A. R. Ruyack, J. W. Kevek, B. Kobrin, D. A. Muller, *Nature* **2015**, *524*, 204.
- [36] S. Babaei, J. Shim, J. C. Weaver, E. R. Chen, N. Patel, K. Bertoldi, *Adv. Mater.* **2013**, *25*, 5044.
- [37] S. Shan, S. H. Kang, J. R. Raney, P. Wang, L. Fang, F. Candido, J. A. Lewis, K. Bertoldi, *Adv. Mater.* **2015**, *27*, 4296.
- [38] S. Xu, Z. Yan, K.-I. Jang, W. Huang, H. Fu, J. Kim, Z. Wei, M. Flavin, J. McCracken, R. Wang, A. Badesa, Y. Liu, D. Xiao, G. Zhou, J. Lee, H. U. Chung, H. Cheng, W. Ren, A. Banks, X. Li, U. Paik, R. G. Nuzzo, Y. Huang, Y. Zhang, J. A. Rogers, *Science* **2015**, *347*, 154.
- [39] Z. Yan, F. Zhang, J. Wang, F. Liu, X. Guo, K. Nan, Q. Lin, M. Gao, D. Xiao, Y. Shi, Y. Qiu, H. Luan, J. H. Kim, Y. Wang, H. Luo, M. Han, Y. Huang, Y. Zhang, J. A. Rogers, *Adv. Funct. Mater.* **2016**, *26*, 2629.
- [40] S. Park, D. Hah, *Sens. Actuators, A* **2008**, *148*, 186.
- [41] R. Johnstone, D. Sameoto, M. Parameswaran, *J. Microeng. Microeng.* **2006**, *16*, N17.
- [42] R. Johnstone, A. Ma, D. Sameoto, M. Parameswaran, A. Leung, *J. Microeng. Microeng.* **2008**, *18*, 045024.
- [43] S.-H. Tsang, D. Sameoto, I. Foulds, R. Johnstone, M. Parameswaran, *J. Microeng. Microeng.* **2007**, *17*, 1314.
- [44] H. E. Jeong, M. K. Kwak, K. Y. Suh, *Langmuir* **2010**, *26*, 2223.
- [45] J. Purtov, M. Frensemeier, E. Kroner, *ACS Appl. Mater. Interfaces* **2015**, *7*, 24127.
- [46] Y. Klein, E. Efrati, E. Sharon, *Science* **2007**, *315*, 1116.
- [47] Z. J. Wang, W. Hong, Z. L. Wu, Q. Zheng, *Angew. Chem., Int. Ed. Engl.* **2017**, *56*, 15974.
- [48] J. Kim, J. A. Hanna, M. Byun, C. D. Santangelo, R. C. Hayward, *Science* **2012**, *335*, 1201.
- [49] Z. L. Wu, M. Moshe, J. Greener, H. Therien-Aubin, Z. Nie, E. Sharon, E. Kumacheva, *Nat. Commun.* **2013**, *4*, 1586.



- [50] M. Pezulla, S. A. Shillig, P. Nardinocchi, D. P. Holmes, *Soft Matter* **2015**, *11*, 5812.
- [51] Q. Ge, C. K. Dunn, H. J. Qi, M. L. Dunn, *Smart Mater. Struct.* **2014**, *23*, 094007.
- [52] S. Naficy, R. Gately, R. Gorkin, H. Xin, G. M. Spinks, *Macromol. Mater. Eng.* **2017**, *302*, 1600212.
- [53] L. Yin, R. Kumar, A. Karajic, L. Xie, J.-M. You, D. Joshua, C. S. Lopez, J. Miller, J. Wang, *Adv. Mater. Technol.* **2018**, *3*, 1800013.
- [54] T. McMillen, A. Goriely, *J. Nonlinear Sci.* **2002**, *12*, 241.
- [55] M. Pezulla, G. P. Smith, P. Nardinocchi, D. P. Holmes, *Soft Matter* **2016**, *12*, 4435.
- [56] S. Timoshenko, *JOSA* **1925**, *11*, 233.
- [57] B. Shin, J. Ha, M. Lee, K. Park, G. H. Park, T. H. Choi, K.-J. Cho, H.-Y. Kim, *Sci. Rob.* **2018**, *3*, eaar2629.
- [58] S. Shian, K. Bertoldi, D. R. Clarke, *Adv. Mater.* **2015**, *27*, 6814.
- [59] S. Liu, Z. Yao, K. Chiou, S. I. Stupp, M. O. de la Cruz, *Proc. Natl. Acad. Sci. USA* **2016**, *113*, 7100.
- [60] O. G. Schmidt, K. Eberl, *Nature* **2001**, *410*, 168.
- [61] D. Y. Khang, H. Jiang, Y. Huang, J. A. Rogers, *Science* **2006**, *311*, 208.
- [62] J. M. McCracken, S. Xu, A. Badea, K. I. Jang, Z. Yan, D. J. Wetzel, K. Nan, Q. Lin, M. Han, M. A. Anderson, J. W. Lee, Z. Wei, M. Pharr, R. Wang, J. Su, S. S. Rubakhin, J. V. Sweedler, J. A. Rogers, R. G. Nuzzo, *Adv. Biosyst.* **2017**, *1*, 1700068.
- [63] R. W. Ogden, *Non-Linear Elastic Deformations*, Ellis Horwood, Hemel Hempsted, UK **1984**.
- [64] A. F. Bower, *Applied Mechanics of Solids*, CRC Press, Boca Raton, FL **2009**.
- [65] J. Shintake, V. Cacucciolo, D. Floreano, H. Shea, *Adv. Mater.* **2018**, e1707035.